${\it Limnol.~Oceanogr.:~Methods~10,~2012,~1078-1095} \\ ©~2012,~by~the~American~Society~of~Limnology~and~Oceanography,~Inc.}$

A multi-tracer model approach to estimate reef water residence times

A. Venti^{1*}, D. Kadko¹, A. J. Andersson², C. Langdon¹, and N. R. Bates³

¹University of Miami, Rosenstiel School of Marine and Atmospheric Sciences, 4600 Rickenbacker Cswy, Miami FL, 33149 ²Scripps Institution of Oceanography, University of California San Diego, 9500 Gilman Dr., La Jolla, CA 92093-0202 ³Bermuda Institute of Ocean Sciences (BIOS), 17 Biological Station Lane, Ferry Reach, Bermuda, GE01

Abstract

We present a new method for obtaining the residence time of coral reef waters and demonstrate the successful application of this method by estimating rates of net ecosystem calcification (NEC) at four locations across the Bermuda platform and showing that the rates thus obtained are in reasonable agreement with independent estimates based on different methodologies. The contrast in 7 Be activity between reef and offshore waters can be related to the residence time of the waters over the reef through a time-dependent model that takes into account the rainwater flux of 7 Be, the radioactive half-life of 7 Be, and the rate of removal of 7 Be on particles estimated from 234 Th. Sampling for 7 Be and 234 Th was conducted during the late fall and winter between 2008 and 2010. Model results yielded residence times ranging from 1.4 (\pm 0.7) days at the rim reef to 12 (\pm 4.0) days closer to shore. When combined with measurements of salinity-normalized total alkalinity anomalies, these residence times yielded platform-average NEC rates ranging from a maximum of 20.3 (\pm 7.0) mmolCaCO₃ m⁻² d⁻¹ in Nov 2008 to a minimum of 2.5 (\pm 0.8) mmolCaCO₃ m⁻² d⁻¹ in Feb 2009. The advantage of this new approach is that the rates of NEC obtained are temporally and spatially averaged. This novel approach for estimating NEC rates may be applicable to other coral reef ecosystems, providing an opportunity to assess how these rates may change in the context of ocean acidification.

Knowledge of net ecosystem calcification rates (NEC = gross calcification – gross calcium carbonate dissolution) is becoming increasingly vital as the percentage of live coral cover on many coral reefs around the world gets steadily lower (Waddell and Clarke 2008; Wilkinson and Bernard 2012). The region-wide average in the Caribbean is now less than 10% (Gardner et al. 2003). This decline raises two critical questions: 1) what is the rate of NEC on these reefs today that used to have coral cover on the order of 50% just 30 years ago? and 2)

*Corresponding author: E-mail: aventi@rsmas.miami.edu

Acknowledgments

The authors would like to thank the following people for their contributions to this work: Dr. Mark Stephens of the University of Miami, Rosenstiel School of Marine and Atmospheric Sciences, for his valuable contributions both in the field and lab; Drs. Michael Lomas and Rod Johnson, chief scientists of the Bermuda Atlantic Time Series (BATS) project; Dafydd Gwyn Evans for his assistance with off-shore sampling, the captain and crew of the R/V Atlantic Explorer, and comments from one anonymous reviewer whose suggestions helped improve this manuscript. This work was supported by the National Science Foundation (NSF) grants OCE0825578 (CL and DK) and OCE0928406 (AJA and NRB).

DOI 10.4319/lom.2012.10.1078

at what point will coral and algal calcification rates fall below the minimum required to keep up with natural rates of loss of calcium carbonate (CaCO₃) on reefs due to bioerosion and dissolution, i.e., are we approaching a tipping point beyond which maintenance of the reef framework will be impossible?

Coral reefs in the Caribbean have experienced a dramatic decline in coral abundance for many reasons including disease, overfishing, die-offs of a key grazer, sedimentation, and eutrophication from coastal development and mortality resulting from bleaching following unusually hot summers (Glynn 1990; Pandolfi et al. 2005; Baker et al. 2008). To this long list should now be added the threat of the steadily increasing acidity of the ocean.

Specifically, the oceanic uptake of anthropogenic CO_2 shifts the equilibrium of carbonate species, increasing the concentration of bicarbonate ions (HCO_3^-), decreasing carbonate ions (CO_3^{2-}), and ocean pH in a series of acid-base dissociation reactions (e.g., Butler 1992; Zeebe and Wold-Gladrow 2001).

$$CO_{2(30)} + H_2O \Leftrightarrow H_2CO_3 \Leftrightarrow HCO_3^- + H^+ \Leftrightarrow CO_3^{2-} + 2H^+$$
 (1)

These trends have been observed in ocean time-series studies in Bermuda and Hawaii (Bates 2007; Orr et al. 2011; Bates

et al. 2012). Studies have shown that a decline in carbonate saturation state associated with a decrease in pH of as little as 0.2-0.3 units can significantly impede coral recruitment and stunt the growth of juvenile and adult corals, seriously impacting their ability to compete for space and light with pH-tolerant species such as macroalgae and sponges (e.g., Langdon and Atkinson 2005; Hoegh-Gulberg et al. 2007; Andersson et al. 2011).

Whereas natural diurnal and seasonal variability of pH in reef environments, typically ranging between 0.5-0.1 units, make it difficult to observe the impact of the 0.1 unit decline that reefs have experienced over the last 200 years, the steadily increasing rate of change over the next 50-100 years will push the pH well outside the historical range (Kayanne et al. 2005; Yates et al. 2007; Gray et al. 2012). Projections indicate a 100% to 150% higher ocean acidity by 2100 (IPCC 2007). It is therefore highly desirable that measurements of NEC become a common component of coral reef health assessments. It is also important that multi-national, time-series studies of NEC and seawater carbonate chemistry be established at several locations in the Caribbean, Indian, and Pacific Oceans, as soon as possible so that baselines can be established against which future changes can be determined.

The measurement of NEC for the purposes of detecting a change due to ocean acidification presents some difficult challenges. The natural diurnal pH signal typically ranges from 0.05-0.1 units for reef ranging between 3-7 m as seen by Yates et al. (2007) in Florida Bay where the authors measured a diurnal pH range between 0.07-0.11units. Recently, however, several studies have revealed more dynamic diurnal pH signals. For example, Gray et al. (2012) found a diurnal pH range of 7.89-8.17 ($\Delta 0.28$) at Media Luna Reef, Puerto Rico. Similarly, Hofmann et al. (2011) measured a diurnal pH range of 0.253 units at Palmyra Reef Terrace, French Polynesia. Other studies have reported even more extreme diurnal pH fluctuations such as Kayanne et al. (2005), who report an average diurnal pH range from 7.9-8.4 ($\Delta 0.5$) and Manzello (2010) who reports a diurnal range of 7.65-8.6 ($\Delta 0.61$) in upwelling impacted reefs of the eastern tropical Pacific.

Further complicating matters is that NEC varies with light and temperature on a diurnal and seasonal basis. Less well understood are other factors like nutrient concentration and food availability that are also known to impact rates of calcification. Detecting a long-term trend in NEC and being able to determine whether or not it can be attributed to ocean acidification will require many years of data. Recall that almost 20 years of data were needed before it was possible to conclusively say that the carbonate chemistry at the oceanic timeseries stations in Hawaii and Bermuda was responding to the rise in atmospheric CO_2 (Bates 2007; Dore et al. 2009; Bates et al. 2012).

Initiatives to establish a comprehensive time series of NEC rates have not yet been established. Previous studies quantifying coral calcification have focused on small spatial scales,

measuring calcification rates of individual coral colonies through x-ray imaging analysis of slabbed coral cores (Chalker et al. 1985; De'ath et al. 2009) or staining colonies with a calcein or alizarin dye (Dikou 2009; Brahmi et al. 2010). Though these methods lend themselves to monthly-annual resolutions, they are limited in their ability to accurately estimate the response of the entire reef community.

A long-term study of community calcification rates has been measured by Silverman et al. (2012) at One Tree Island reef, adopting the stagnant water method used by Don Kinsey in the 1970s and 1980s. This study reports a steady decline in NEC over the last 40 years, however results obtained by this method may not be generalizable to the more typical high energy reef environments. It is possible that the decline Silverman reports (i.e., high rates of bioerosion and dissolution) are unique to the low energy environments, which might also collect and retain organic matter that would stimulate the growth of bioeroders. Thus there remains a need to develop a method to measure NEC rates in a wide range of environments.

One method to determine calcification rates over a range of spatial and temporal scales (from individual coral colonies to coral reef communities, and from hours to months) is the alkalinity anomaly method (Smith 1973; Langdon et al. 2010), whereby the production of ${\rm CaCO}_3$ is determined from the observed decrease in total alkalinity (TA) of the surrounding seawater. The net calcification rate is given by

$$G = -0.5 \ \rho_{w} \frac{\Delta T A z}{\Delta t} \tag{2}$$

where G is the calcification rate in mmolCaCO₃ m⁻² per unit time, ρ_w is the density of seawater (kg m⁻³), $\Delta TA/\Delta t$ is the time rate of change in TA (µmol kg⁻¹), and z is the depth of the water (m). The alkalinity anomaly method is appropriate for experiments involving individual coral colonies with short incubation times (hours, Gattuso et al. 1998; Schneider and Erez 2006), mesocosm studies (Langdon et al. 2003; Langdon and Atkinson 2005; Andersson et al. 2009), and in situ reef studies (Wantanabe et al. 2006; Silverman et al. 2007). To derive NEC rates for these large-scale community experiments, the observed alkalinity anomaly is divided by average reef water residence time (τ) , which reflects the mean amount of time a water parcel resides in the system before being flushed with offshore water. Residence time is not simply the time it takes a parcel of water to transit a system, i.e., the linear dimension divided by the current speed. A good example to highlight this difference would be the Florida Keys where eddies and wind-driven recirculation cells return water parcels back onto the reef many times before they escape the system, even though the system would appear to have an open boundary with the ocean (Haus et al. 2000). In this situation, the residence time can be many times the 12 hours tidal cycle.

Though analytical methods for measuring TA are well established, accurate estimates of reef water residence times

have been historically difficult to quantify, thereby limiting the application of the alkalinity anomaly method for estimating NEC rates (e.g., Delesalle and Sournia 1992; Andréfouët, et al. 2001). Earlier studies often relied on the salinity difference between offshore and onshore waters to estimate residence times within a reef system (e.g., Smith and Pesret 1974; Smith and Jokiel 1978). Although this approach is effective for estimating longer residence times of weeks to months commonly found in bays, atolls, and lagoon environments, the salinity method has low precision for residence times less than a few days due to minimal salinity gradients between off-shore and reef waters. For typical conditions, the observed difference in salinity between offshore and onshore reef waters is approaching the detection limit of the sensor (however see Silverman et al. 2007 who used the method to obtain residence times in the Red Sea in the range of 4-6 h). In addition, the difference in evaporation and precipitation (E-P) is often not known with any precision for specific locations and dates. In Bermuda, the lack of sufficient E-P data and minimal difference between off shore and reef water salinity (difference between offshore and reef water salinity averaged < 0.18 during this study, n = 102) results in large uncertainties in estimated residence times, and thus cannot be confidently used to estimate NEC.

In this article, we present a new method to estimate reef water residence times based on the difference in beryllium-7 (7Be) activities between offshore and reef waters. 7Be is a naturally occurring, cosmogenic radionuclide whose half-life of 53.3 days provides a timescale suitable for reef environments with residence times ranging from a day to several weeks. After using the new method to measure the residence times of reef waters on the Bermuda platform, we compare our residence times with earlier estimates based on a hydrodynamic circulation model. We also apply the alkalinity anomaly-residence time method to determine rates of NEC and compare the rates thus obtained to rates reported in the literature.

Background

Beryllium-7 enters the ocean via precipitation and is subsequently homogenized within the surface mixed layer (e.g., Silker 1972; Kadko and Olson 1996). The production rate of ⁷Be in the troposphere depends on altitude, geomagnetic latitude, and an 11-y period solar cycle (Sakurai et al. 2005). Over shorter timescales, seasonal variability of ⁷Be flux in rainfall has also been observed (Akata et al. 2007). Across broad oceanic regions (1000s km), the ⁷Be inventory from rain varies as a function of rainfall, and mixed layer inventories are inversely related to salinity (Kadko and Olson 1996). On smaller scales (100s km), the mixed layer depth is a critical parameter that largely determines the ⁷Be surface activity; a given inventory is diluted over deep mixed layers and concentrated within shallow mixed layers.

Of relevance to the present application, the open ocean inventory of ⁷Be is diluted throughout the mixed layer, typically 142-175 m in the winter months (Nov–Mar) and occasionally reaching over 400 m, though shallower in the sum-

mer months (Jul–Sep 11 - 65 m), whereas the same inventory is concentrated over adjacent shallower reef platform, typically 8-18 m (http://bats.bios.edu/bats_form_ctd.html). This results in higher ⁷Be activities over the reef as compared with the offshore water. The persistence of this contrast in ⁷Be activity between the open-ocean and reef platform can be used to estimate the residence time of water over the reef. For example, a high exchange rate, or short residence time, would tend to diminish this contrast in ⁷Be activity.

Previous studies have used ⁷Be to trace short time scale ocean phenomena such as deposition of sea ice-rafted material (Cooper et al. 2005), Arctic mixed layer evolution (Kadko 2000), and oxygen use (Kadko 2009). The inherent ability of ⁷Be to trace events on short timescales (days to weeks) lends itself to determining residence times for many reef environments.

Materials and procedures

Study sites

Four study sites, anticipated to have different residence times, were selected for observational studies (Fig. 1). Previous estimates of reef water residence times for the Bermuda reef system were based on a physical circulation model, which incorporated tides and wind mixing (R. Johnson unpub. data). Briefly, this model implemented the general purpose European Continental Shelf Model (Prandle 1984) and was calibrated for the Bermuda reef system with the support of current meter data. Boundary conditions were principally forced by eight of the major diurnal and semi-diurnal tidal constituents which account for > 95% of the tidal variance in Bermuda.

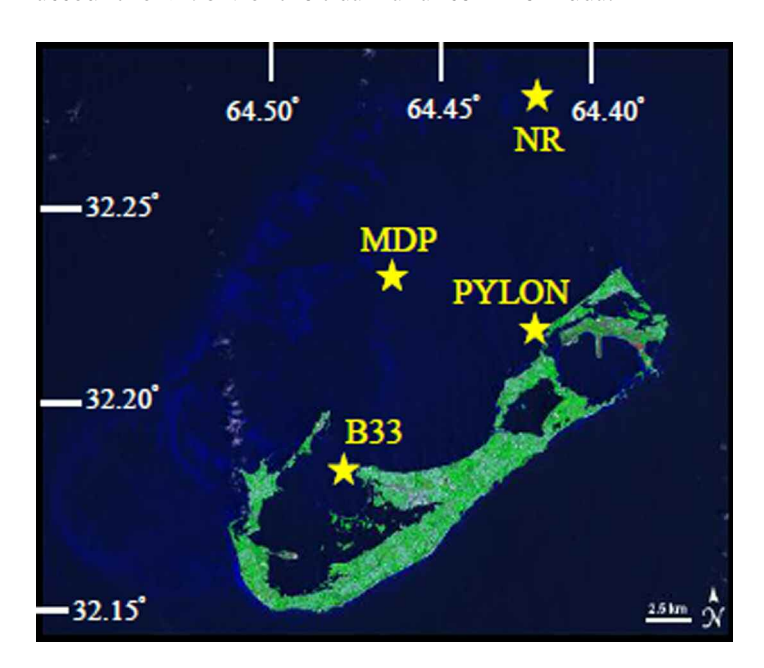


Fig. 1. Location of the 4 study sites across the Bermuda reef platform. NR is expected to have the shortest residence time, due to its proximity to the platform edge. B33, isolated within the western lagoon, is expected to have the longest residence time. (Google™ Earth)

The sites selected for the present study include (1) Buoy 33 (B33, 32.32203°N 64.811718°W), which based on a previous modeling study (R. Johnson unpub. data) was expected to have a relatively long residence time (8-10 d), (2) mid-platform (MDP, 32.37218°N 64.78143°W), and (3) Pylon (32.364516°N 64.71573°W), both with anticipated intermediate residence times of 3-5 d and (4) North Rock (NR, 32.473247°N 64.74572°W), likely with a short residence time of only 1-3 d. Fall and winter samplings were conducted at these four sites between Nov 2008 and Mar 2010. Reef water samples were not collected directly over the reef, but rather in-between reefs and thus represent the integrated signal of each study site.

Analytical methods

Atmospheric flux of ⁷Be

The atmospheric flux of ${}^7\text{Be}$ was estimated from rainwater samples collected from the island of Bermuda at the BIOS research station over known time periods. It has been shown that the flux of ${}^7\text{Be}$ estimated in this manner matches that required to sustain the ocean inventory of ${}^7\text{Be}$ observed at the nearby Bermuda Atlantic Time Series (BATS) and Hydrostation S sites (Kadko and Prospero 2011). Samples were spiked with 0.5 mL stable Be standard and 2-3 mL of iron chloride (FeCl₃). The ${}^7\text{Be}$ was then coprecipitated with iron hydroxide by adding NaOH and the precipitate was dried, powdered, and homogenized in plastic Petri dishes. Samples were analyzed for ${}^7\text{Be}$ using a low background germanium ${}^{\gamma}$ detector by integration of its peak at 478KeV. Atomic absorption analysis of stable Be in the precipitate determined the overall chemical yield (Kadko 2000).

Seawater ⁷Be activities and supporting measurements.

To determine 7Be in reef and open ocean water 200 L surface water samples were pumped through iron-impregnated acrylic filters twice (Lee et al. 1991). The efficiency of the fiber for extraction of Be from seawater was predetermined by adding 500 mL of a 1000 ppm Be atomic absorption standard to a drum containing 700 L of sea water. Seawater was pumped through an iron fiber cartridge and at every 100 L the Be content of the cartridge effluent was measured by atomic absorption. From this data, the integrated Be extraction efficiencies were calculated based on the volume of water sampled (i.e., 100-700 L in 100 L increments) and typically ranged from 76% to 82% for each water volume sampled. After filtration, fibers were dried, ashed, compressed into 5.8 cm diameter pellets (Kadko and Olson 1996; Kadko 2000) and placed on a low background germanium γ detector.

Particulate matter was filtered from approximately 200 L of reef water using GF/F under vacuum and analyzed for both ⁷Be and ²³⁴Th. Filters were spiked with 0.5 mL of stable Be and ²³⁰Th standards, dissolved in 70% nitric acid, and spiked with 2-3 mL iron chloride before being split for separate ⁷Be and ²³⁴Th analysis. ⁷Be particle samples were processed in a manner identical to the rainwater samples described above.

²³⁴Th was analyzed on particle samples, as well as 10 L seawater samples. As with the filter samples, seawater samples

were spiked with 230 Th and precipitated with iron chloride and sodium hydroxide. Both particle and seawater samples were subsequently taken up in 8N HCl and processed according to methods discussed elsewhere (e.g., Bhat et al. 1969; Coale and Bruland 1985). Briefly, after purification by anion exchange chromatography, samples were plated by electro-deposition onto 1 inch stainless steel disks to determine 234 Th by β counting, and 230 Th, (for overall chemical yield) by α counting. β efficiency was 48% and α efficiency ranged from 25.1% to 29.2%. In all cases, uncertainties in the detector efficiency were smaller than the statistical counting error and background.

Surface seawater samples for TA were sampled by hand into clean 200 mL Kimax borosilicate glass bottles and poisoned with 100 μL of saturated ${\rm HgCl_2}$ solution to prevent any biological alteration (Bates et al. 1996a). Samples were returned to BIOS where TA was determined by potentiometric titration with HCl according to Bates et al. (1996a 1996b). Calibration standards were within 0.15% (~2-3 $\mu mol~kg^{-1}$) of certified TA values reported by A. G. Dickson (http//www.dickson.ucsd.edu, Dickson et al. 2003).

Model description

Beryllium-7 can be used as a tracer for reef water residence time if all the sources and sinks to the reef system are accounted for. With no river or significant ground water input, there are two sources of ⁷Be to the reef: (1) rainwater input, and (2) exchange with offshore water. There are three loss terms of ⁷Be from the reef system to consider: (1) radioactive decay, (2) exchange to offshore water, and (3) particle removal. This model is represented by the box diagram in Fig. 2.

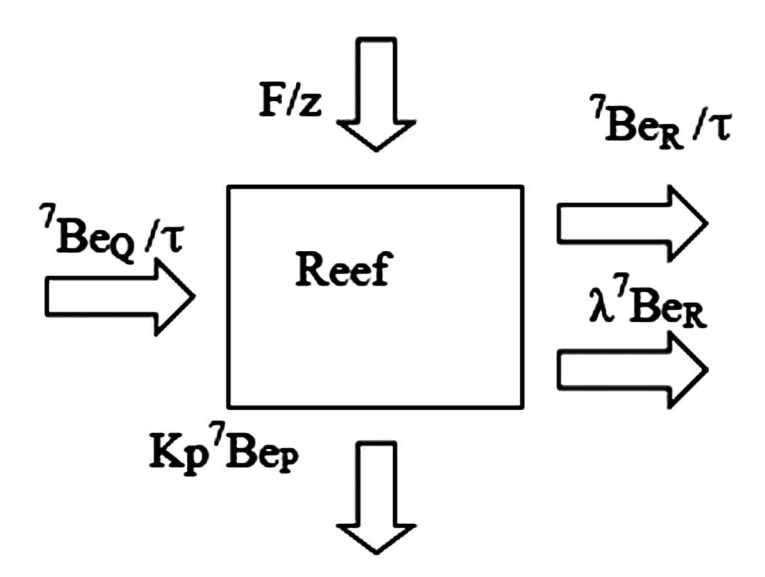


Fig. 2. A schematic drawing of the ⁷Be model over a coral reef. F = the flux of ⁷Be into the system (dpm m⁻² d⁻¹); z = the reef depth (m); ⁷Be_Q = the activity of ⁷Be in the open ocean (dpm m⁻³); ⁷Be_R = the activity of ⁷Be over the reef (dpm m⁻³); λ = the decay constant of ⁷Be, 0.013 d⁻¹; ⁷Be_P = the activity of ⁷Be on particles (dpm m⁻³); and Kp = the particle removal rate constant (d⁻¹).

Under steady state the ⁷Be budget can be expressed as:

$$\frac{F}{7} + \frac{{}^{7}Be_{Q}}{\tau} = \frac{{}^{7}Be_{R}}{\tau} + \lambda^{7}Be_{R} + K_{p}{}^{7}Be_{p}$$
 (3)

where 7Be_Q , 7Be_R , and 7Be_p are, respectively, the activities of 7Be in offshore water, reef water, and particulate matter (dpm m⁻³), F is the rainwater flux of 7Be into the system (dpm m⁻² d⁻¹), z is the average reef platform depth (m), Kp is the particle removal constant (d⁻¹), τ is the residence time (d), and λ is the decay constant for 7Be (0.013 d⁻¹). All model variables are based on measurements, except Kp and τ , generating a model with one equation and two unknowns.

A second tracer, thorium-234 (234Th), is required to resolve the model. 234 Th is a short lived ($t_{1/2} = 24.1$ d) particle reactive radionuclide. Disequilibria between ²³⁴Th and its parent ²³⁸U have often been used as a tracer of particle dynamics in marine environments (e.g., Broecker et al. 1973; Muir et al. 2005). It is important to note that ²³⁴Th is used to estimate the sinking rate of particles (Kp), not the flux of 7Be from particles, because we cannot assume that ⁷Be and ²³⁴Th have the same particle affinity. To sidestep this unknown, the scavenging rate (Kp) is multiplied by the activity of ⁷Be measured on filtered particles thus providing an estimate of the ⁷Be flux from particle scavenging. This method is appropriate for determining rates occurring over timescales of days to months, thus providing a suitable tracer for a model estimating residence times in dynamic reef environments (Moran et al. 2003). For the purposes of this model, particle suspension from the sediment is ignored, thus the model does not account for 7Be or 234Th previously lost to the sediment, but rather incorporates only the flux from particles during the time period for which the model is run.

The ²³⁴Th budget across the reef can be represented by a box model (Fig. 3) in a fashion similar to that of ⁷Be. At steady state:

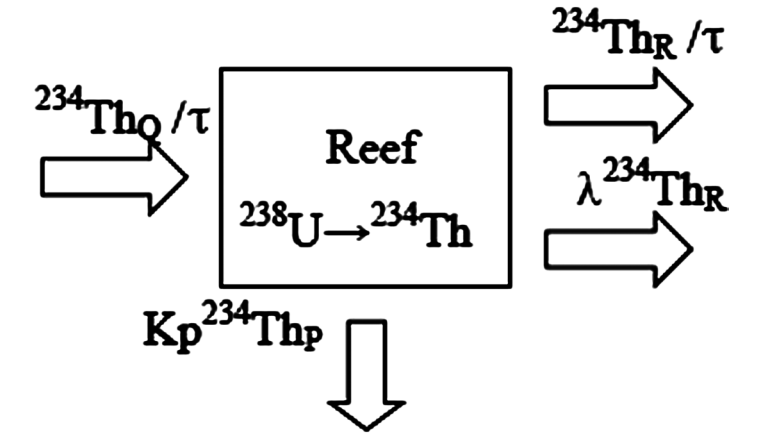


Fig. 3. A schematic drawing of the 234 Th model over a coral reef. 234 Th $_Q$ = the activity of 234 Th in the open ocean (dpm m $^{-3}$); 234 Th $_R$ = the activity of 234 Th over the reef (dpm m $^{-3}$), $_-$ = the decay constant of 234 Th, 0.02876 d $^{-1}$; 234 Th $_P$ = the activity of 234 Th on particles (dpm m $^{-3}$); and Kp = the particle removal rate constant (d $^{-1}$).

$$\frac{^{234}Th_{Q}}{\tau} + \lambda^{238}U = \frac{^{234}Th_{R}}{\tau} + \lambda^{234}Th_{R} + Kp^{234}Th_{P}$$
 (4)

where $^{234}Th_Q$ $^{234}Th_R$, and $^{234}Th_p$ are the activities of ^{234}Th in offshore water, reef water, and particulate matter respectively (dpm m $^{-3}$), $\lambda^{238}U$ is the production term of ^{234}Th from uranium, Kp is the particle removal rate constant (d $^{-1}$), τ is the residence time (d), and λ is the decay constant for ^{234}Th (0.02876 d $^{-1}$). All model parameters can be measured except Kp and τ . With two Eqs. 3 and 4 and two unknowns, we can now solve for Kp and τ analytically.

Though useful in concept, there are two issues with the steady state box model to consider. First, the "box" in question assumes a well-mixed uniform reservoir and must therefore be clearly defined. This could refer to the entire reef platform, where the platform is represented by average parameters (Kp and τ). Alternatively, the box could represent each study site characterized by its own independent set of parameters. The "footprint" or spatial range encompassed within these boxes is dependent on the tracer response times. These response times, if controlled solely by the radioactive mean life of these tracers, would be on the magnitude of tens of days (response time = λ^{-1} which corresponds to 35 and 75 d for ²³⁴Th and ⁷Be, respectively). However, in the coral reef environment of the present study, these tracers are also heavily influenced by particle removal (Kp), which results in a much shorter tracer response time, on the order of days.

Response Time =
$$(\lambda + Kp)^{-1}$$
 (5)

If the tracer response time and the anticipated residence time at each study site are on the same order of magnitude then consideration of a more narrowly defined box (that is, a box which encompasses individual sites rather than the entire reef platform) could be justified. This study considers both platform-average and site-specific analyses.

Second, the assumption that the system is at steady state may not be valid over long time periods in high-energy reef environments during which, for example, residence time and particle sequestration may vary. However, for shorter periods, comparable to the tracers' response time, the steady state assumption (i.e., a constant Kp and residence time) may be appropriate. To evaluate this issue, Eqs. 3 and 4 are presented in the non-steady state form to consider how ⁷Be and ²³⁴Th change over time. Eq. 3 therefore becomes:

$$\frac{d^7 Be}{dt} = \frac{F}{z} + \frac{^7 Be_Q}{\tau} - \lambda^7 Be_R - K_p^{7} Be_P - \frac{^7 Be_R}{\tau} \tag{6}$$

and Eq. 4 becomes:

$$\frac{d^{234}Th}{dt} = \frac{^{234}Th_{Q}}{\tau} + \lambda^{238}U - \lambda^{234}Th_{R} - K_{p}^{234}Th_{P} - \frac{^{234}Th_{R}}{\tau}$$
(7)

Utilizing the STELLA modeling software, the two box models (Figs. 2 and 3) were constructed with reef water ⁷Be and

²³⁴Th activities described by Eqs. 6 and 7. Initially the box was defined as the entire reef platform by using the average of the parameter values (${}^{7}\text{Be}_{\text{p}}$, ${}^{234}\text{Th}_{\text{p}}$) measured across the platform. The box was then redefined to represent the individual study sites by using the measured data from each site. Since water samples were collected adjacent to reefs, these site-specific data represent the integrated signal for each study site, an area defined by the model's "footprint" (discussed below). Each model run was initialized with a reef water ${}^{7}\text{Be}$ and ${}^{234}\text{Th}$ activity defined by the offshore value, and run at incremental Δt of 0.25 d. A sensitivity analysis was applied with Kp values ranging from 0.02 to 1.0 (Savoye et al. 2006) and an initial residence time of 1 d, which increased systematically by 1 d in subsequent model runs. Taking into consideration tracer response times, models were run for 25 d.

Model output reef water ^7Be and ^{234}Th activities were then compared with the data to determine which Kp-residence time combinations simultaneously yielded the measured activities of both tracers. For each sampling period analyzed by the model there existed one solution (i.e., one Kp and residence time combination) that simultaneously best fit both time-dependent models. To assess the model's precision, we look at the effects of analytical uncertainty of each measured parameter on the overall uncertainty of Kp and τ . We also evaluate the model's sensitivity to Kp, τ and λ , to better understand what parameters are impacting the system.

Assessment and discussion

Distribution of parameters across the Bermuda reef platform

TA, ⁷Be, and ²³⁴Th measured over the four study periods, Nov 2008, Feb 2009, Nov 2009, and March 2010, are plotted as a function of their position from the platform edge at North Rock (Fig. 4 A-D). The least mean square exponential fits of the data are also shown and were used to estimate the mean platform value for each of the measured parameters (Table 1).

Generally, the distribution expected for each tracer was observed, with characteristics of newly flushed water near the platform edge and 'aged' (that is, isolated with respect to offshore influence) water near-shore. Specifically, the activity of ⁷Be in reef water increased across the reef platform as a function of distance from the edge. This reflects the accumulation of atmospheric ⁷Be input as water 'aged' toward shore, which is also reflected in the activities of particulate ⁷Be. ²³⁴Th, on the other hand, decreased across the reef platform as a result of cumulative scavenging as the water aged.

Seasonal differences in TA distribution across the Bermuda reef platform were also evident. November data, both 2008 and 2009, showed depletion in TA from the platform edge shoreward (Fig. 4A,C; Table 1). February 2009 showed only a moderate decline compared to November results, whereas in March 2010 TA displayed a slight increase from the platform edge toward shore (Fig. 4B,D). Seasonal differences in TA could arise from seasonal differences in either net calcification rate

(calcification – dissolution; Bates et al. 2010), or reef water exchange rate.

The ⁷Be distribution across the reef can readily distinguish these possibilities, as it serves as a tracer of exchange rate independent of calcification processes. If the higher, uniform TA measured in February and March were a result of faster exchange with offshore waters then the ⁷Be activity over the reef would also be uniform and similar to that of the open ocean. However, ⁷Be activities during all seasons, including February and March, display a gradient across the reef (Fig. 4). This suggests that the high, uniform TA across the reef in February and March resulted from diminished wintertime net calcification rates and not from rapid exchange. In contrast, the lower TA across the reef, with a decreasing gradient relative to offshore water observed in November suggests increased NEC and net CaCO₃ production for that time period.

The ability of ⁷Be to identify seasonal changes in calcification rate as the cause of the observed seasonal TA gradient, and not seasonal changes in exchange rates, can also be seen by plotting TA against ⁷Be for all the stations across the reef platform over each sampling period. Here, the ⁷Be activity across the reef is corrected for particle removal to isolate only the effect of residence time on reef water ⁷Be activity. It can be shown that

corrected
$${}^{7}Be_{R} = measured {}^{7}Be_{R} + \frac{Kp7BeP}{(\tau + \lambda)^{-1}}$$
 (8)

Fig. 5 shows the ⁷Be increases across the reef for every sampling period, whereas TA is constant during February and March and decreases during the November periods.

Average seasonal results for the Bermuda platform

Averaged platform data (Table 1) would be appropriate model inputs under the assumption that the platform is a uniformly mixed system, to yield a single Kp and residence time, which represents a seasonal average for the entire reef platform. The platform-average model generally reproduced ($r^2 > 0.75$) the observed trends in ²³⁴Th and ⁷Be across the reef tract for the 25 d run (Fig. 6). Deviations from the average platform model output may suggest local influences whereby site specific, rather than average data, may be appropriate (discussed in the next section).

The seasonal average platform residence time, derived from the average modeled $^7\mathrm{Be}$ and $^{234}\mathrm{Th}$ activities, ranged from 12 (± 4) days in Feb 2009 to 8 (± 2) days in Nov 2008, falling within the 1-20 d range anticipated for the Bermuda reef system (R. Johnson unpub. data) and manifesting minimal seasonal variation (Fig. 7), though sampling events do not represent the summertime seasonal maxima.

Results from individual study sites

Though the ⁷Be and ²³⁴Th activities predicted by the average model are in good agreement with measured ⁷Be and ²³⁴Th activities from sites distributed across the platform (Fig. 6), apparent deviations might suggest portions of the reef platform are not consistently represented by an average residence

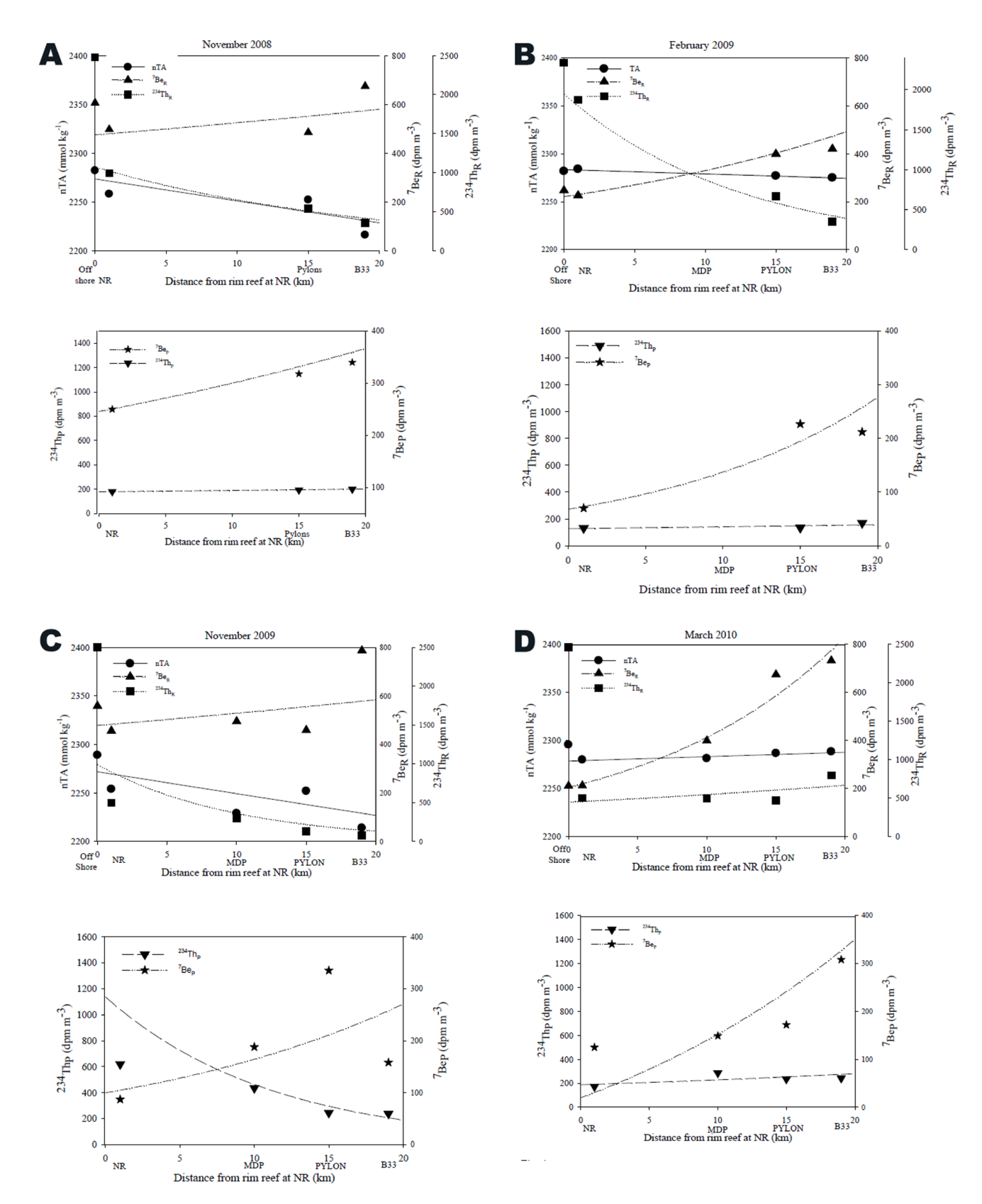


Fig. 4. $^{7}\text{Be}_{\text{R}'}$ $^{7}\text{Be}_{\text{p}'}$ $^{234}\text{Th}_{\text{p}'}$ $^{234}\text{Th}_{\text{p}'}$ nTA (S = 35.00), plotted as a function of position from the platform edge at NR with 0 representing offshore (NR at 1000 m, MDP at 10,000 m, Pylon at 15,000 m, and B33 at 19,000 m), for data collected in Nov 2008 (A), Feb 2009 (B), Nov 2009 (C), and Mar 2010 (D). Points represent collected data; lines indicate the respective least mean square fits.

Table 1. Summary of seasonal average data. Mean data values were calculated by averaging values from the least mean square exponential fit (Fig. 4) extrapolated from 0 to 20,000 m (that is, the approximate distance from the rim reef at NR to B33). TA values are normalized to a salinity of 35.

	nTAª (µmol kg-¹)	r²	⁷ Be _R ^a (dpm m ⁻³)	r²	⁷ Be _p a (dpm m⁻³)	r²	²³⁴ Th _R ^a (dpm m ⁻³)	r²	²³⁴ Th _p ^a (dpm m ⁻³)	r²
Nov 08	2250.92	0.72	525.51	0.38	302.25	1	678.29	0.96	189.87	0.98
Feb 09	2278.94	0.88	338.94	0.98	148.95	0.93	971.94	0.97	141.81	0.67
Nov 09	2249.32	0.62	529.69	0.24	171.38	0.46	428.72	0.90	518.64	0.79
Mar 10	2282.96	0.88	447.18	0.98	165.33	0.77	551.74	0.34	230.56	0.43

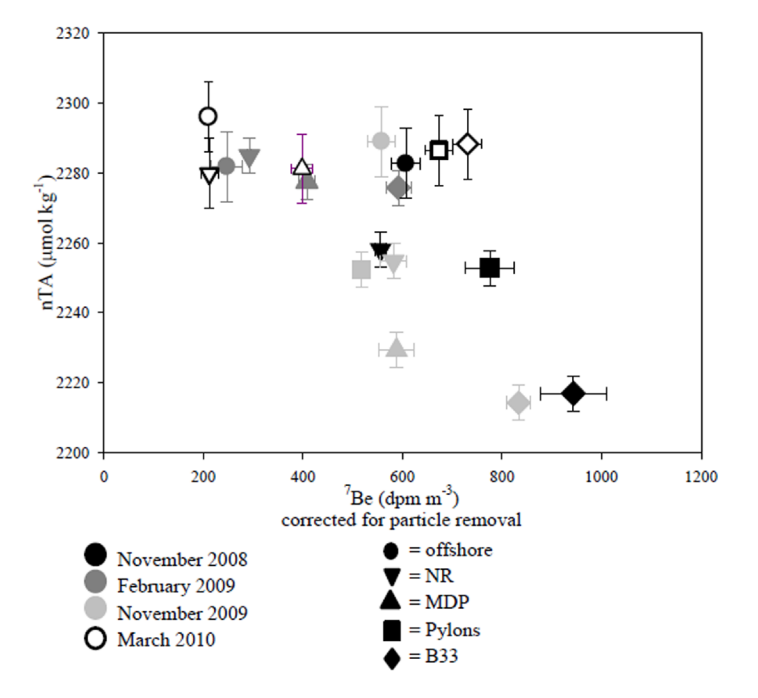


Fig. 5. ⁷Be, corrected for particle removal, plotted against salinity normalized total alkalinity (S = 35). The maintenance of the gradient in ⁷Be across the reef platform between Nov and Feb/Mar provides evidence that the change in nTA is due to seasonal differences in NEC rate and not enhanced wintertime flushing rates. Error bars represent analytical uncertainties.

time. Alternatively, these sites may be significantly influenced by local conditions and better represented by local residence times. To explore this possibility, the model "box" was redefined to represent each study site, thus evaluating the model's ability to estimate site-specific residence times by creating a chain of interconnected box models. In this "serial box model" the residence time of each box is calculated relative to the exchange with the adjacent box, and not offshore waters. The chain is defined by the proximity to the rim reef at NR (NR-MDP-Pylon-B33). Thus at MDP we assume the incoming activity fluxes are defined by the activities measured at NR, for Pylon the input fluxes are defined by the activities measured at MDP, and for B33 the input fluxes are defined by the activities measured at Pylon. The NR box, situated on the platform edge, maintains offshore fluxes under the serial box model.

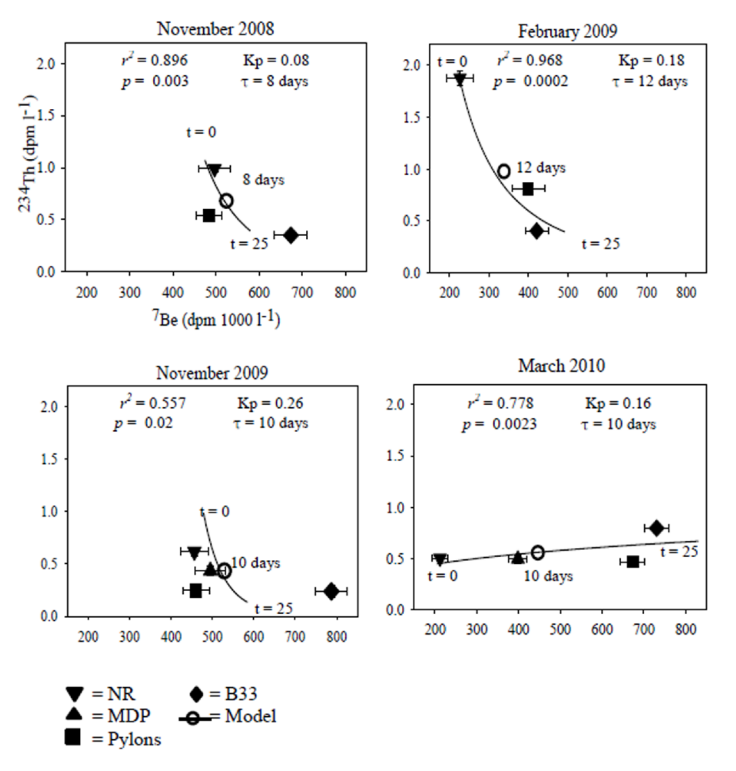


Fig. 6. Reef water 234 Th plotted against reef water 7 Be activities. The closed symbols are measured values; open symbols represent the average platform activities. The model uses the average platform values of 234 Th and 7 Be (Table 1), to yield average Kp and τ for the Bermuda reef platform. Using these parameters the model generates the trend lines shown (from t = 0 to t = 25 days) and indicates the general aging as one moves from the reef edge (NR) to the most isolated station (B33). Deviations from these lines may suggest local infuences among sites.

Overall, site-specific residence times derived from the present model agreed well with previous results obtained by the physical circulation model (R. Johnson, Fig. 7). North Rock displayed the shortest residence times ranging from $1.4 (\pm 0.9)$ days in Nov 2008, to $4.5 (\pm 1.2)$ in Mar 2010, with an average residence time of $2.6 (\pm 1.3)$ days. These results fall within the range of 1-3 days predicted by the physical model for 3 of the 4 sampling periods. Results from B33 were also comparable with those of the physical model. As anticipated, B33 experienced the longest residence time among all sites, ranging from

7 (\pm 2) days in November 2008, to 12 (\pm 4) days in November 2009, with an average residence time of 9.3 (\pm 2.1) days. These results again fell within the range of 8-10 days predicted by the physical model for 3 of the 4 sampling events (Table 2).

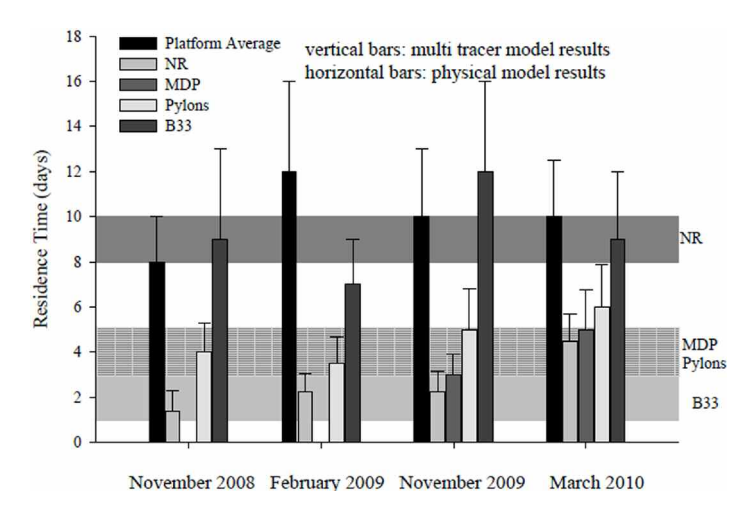


Fig. 7. Season-average and site-specific residence times estimated from the time-dependent model. Vertical bars represent results from the present study. Horizontal bars denote previously estimated residence times of regions encompassing our study sites (R. Johnson, BIOS, unpub. data), and correspond with the like shading pattern of vertical bars. Platformaverage residence times (black vertical bars) are, in most cases, longer than site-specific residence times (shaded vertical bars) as water takes longer to flush over the entire reef platform versus a specific study area, defined by the model footprint.

Despite the general agreement between the physical circulation model and our tracer-based results, differences were observed, with the most notable discrepancies at Pylon and MDP. The hydrographical dynamics of these mid-platform regions are more variable than those of the platform edge (NR), which is continuously flushed with offshore water and therefore has a short residence time, or sheltered lagoons (B33), with a longer residence time due to isolation and distance from the platform edge. It is therefore reasonable that mid-platform sites such as Pylon and MDP experience a broader range of residence times contributing to discrepancies between our results and the circulation model calculations. In addition, these central platform regions are probably influenced by additional circulation complexities compared to boundary regions like NR and B33.

As previously mentioned, it is difficult to compare modeled results with previous estimates of reef water residence times due to the limitations in estimating short time scale reef water residence times. We attempted to verify our results using the salinity anomaly method, but this proved difficult due to the minimal difference between offshore and reef water salinity values and limited evaporation-precipitation (E-P) data. For this analysis, we conducted a platform wide survey in March 2012, and again in September 2012, measuring sea surface salinity at 50 sites distributed across the Bermuda reef platform. Off shore salinity samples were collected at 24 and 28 stations along the cruise transect from Bermuda to the BATS station in Mar and Sep 2012, respectively. With limited cli-

Table 2. Residence times, particle removal rates (Kp), and tracer response times for each study site and sampling period. Tracer response times are on the same order of magnitude and, in most cases, less than the estimated residence time suggesting that these tracers are responding at a timescale suitable for estimating local reef water residence times. Averages represent the platform-average parameter value for each sampling period.

		Residence				⁷ Be response		²³⁴ Th response	
Date	Site	time (d)	±	Kp (d⁻¹)	±	time (d)	±	time (d)	±
Nov 08	Average	8	2	0.08	0.03	10.75	1.51	9.54	1.34
NR	1.40	0.70	0.70	0.28	1.40	0.22	1.38	0.22	
Pylon	4.00	1.30	0.06	0.01	13.70	0.66	11.78	0.57	
B33	9.00	4.00	0.04	0.02	18.87	6.79	15.41	5.55	
Feb 09	Average	12.00	4.00	0.18	0.08	5.18	1.02	4.88	0.96
NR	2.25	0.80	0.25	0.10	3.80	0.61	3.64	0.58	
Pylon	3.50	1.00	0.04	0.01	18.87	0.75	15.41	0.62	
B33	7.00	2.00	0.14	0.04	6.54	0.59	6.07	0.55	
Nov 09	Average	10.00	3.00	0.26	0.09	3.66	0.44	3.51	0.42
NR	2.25	0.90	0.25	0.06	3.80	0.20	3.64	0.19	
MDP	3.00	0.90	0.08	0.02	10.75	0.47	9.54	0.42	
Pylon	5.00	1.80	0.62	0.14	1.58	0.08	1.55	0.08	
B33	12.00	4.00	0.04	0.01	18.87	0.75	15.41	0.62	
Mar 10	Average	10.00	2.50	0.16	0.08	5.78	1.45	5.41	1.35
NR	4.50	1.20	0.50	0.13	1.95	0.13	1.91	0.13	
MDP	5.00	1.75	0.04	0.01	18.87	1.48	15.41	1.21	
Pylon	6.00	1.90	0.08	0.02	10.75	0.78	9.54	0.70	
B33	9.00	3.00	0.12	0.04	7.52	0.87	6.90	0.80	

mate data available, we assumed E-P rates of 4.5 mm d⁻¹ according to data from the European Centre for Medium-Range Weather Forecasts (RCMRWF). Residence times were then estimated according to the salinity anomaly method, defined as:

$$\tau = \frac{z}{(E-P)} \cdot \frac{\left(S_R - S_Q\right)}{S_O} \tag{9}$$

where z is the reef depth (m) E-P is the evaporation minus precipitation rate (m d^{-1}) and S_R and S_Q are the sea surface salinity of reef water and offshore respectively. These data are shown in Table 3.

We averaged all 50 data points to estimate the platform-average residence time. Site-specific residence times were assessed by averaging the data from stations found within the multi-tracer model footprint (discussed below). The results from this effort (Fig. 8, Table 4) yield platform-average residence times that are in close agreement with those estimated from the multi-tracer model, except the uncertainty of the in the salinity based τ is almost twice that of the multi-tracer model. It should be noted, too, that this uncertainty in salinity estimated τ is based only on the uncertainty in salinity measurements as we do not know the uncertainty associated with E-P rates. It is likely that this would contribute greatly to the overall uncertainty in estimated τ .

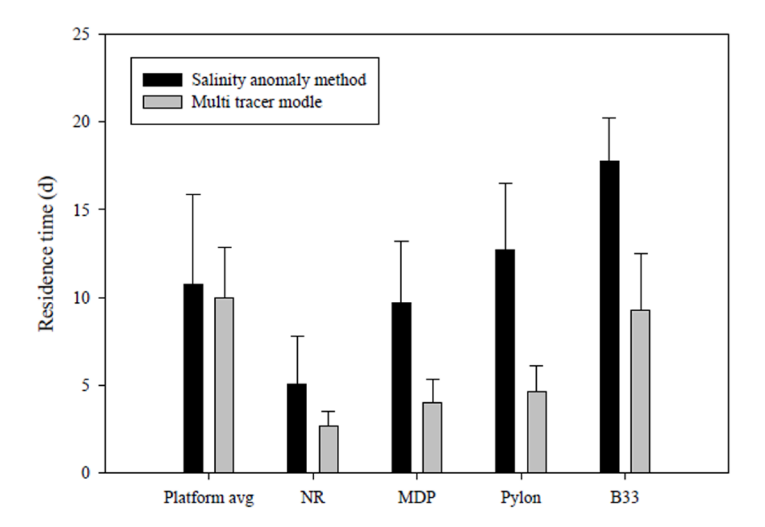


Fig. 8. Platform-average residence times estimated using the salinity anomaly model (black) and multi-tracer model (gray). The agreement between the two methods helps to validate the new multi-tracer model. The greater certainty of the multi-tracer model, compared to the salinity anomaly method, makes it a more ideal method for estimating reef water residence times in the high energy environment of the Bermuda reef platform

Table 3. Offshore and reef water salinity data and E-P rates used to calculate residence times based on the salinity anomaly method.

	Salinity	∆Sal	SD ∆Sal	E-P (m d ⁻¹)	τ (d)	SD τ
Mar 12						
offshore	36.524					
Platform avg	36.706	0.182	0.075	0.0045	11.1	4.5
NR	36.596	0.072	0.022		4.4	1.3
MDP	36.710	0.186	0.048		11.3	2.9
Pylon	36.754	0.230	0.034		14.0	2.1
B33	36.812	0.288	0.010		17.5	0.6
Sep 12						
offshore	36.446					
Platform avg	36.616	0.170	0.095	0.0045	10.4	5.8
NR	36.540	0.094	0.067		5.7	4.1
MDP	36.579	0.133	0.067		8.1	4.1
Pylon	36.634	0.188	0.090		11.5	5.5
B33	36.742	0.296	0.070		18.0	4.3

Table 4. Residence times estimated from the salinity anomaly method and the multi-tracer model with corresponding standard deviations.

	τ salinity (d)	SD τ	τ Be-7 (d)	SD τ	
Platform avg	11	5	10	3	
NR	5	3	3	1	
MDP	10	3	4	1	
Pylon	13	4	5	2	
B33	18	2	9	3	

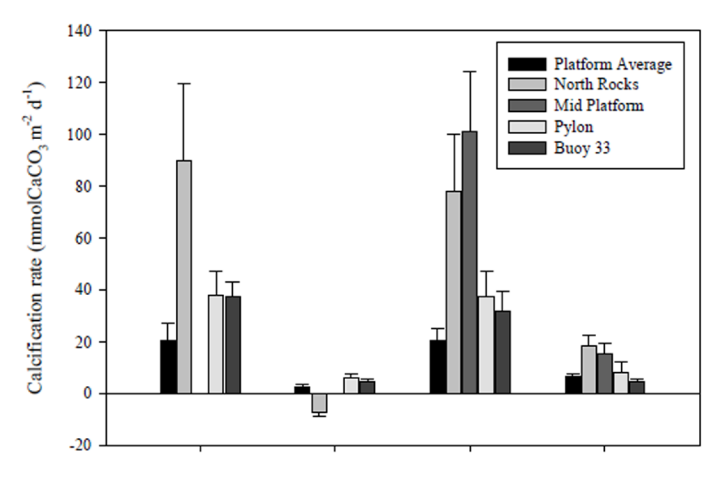
For site-specific residence times however, the multi-tracer model tends to underestimate τ compared with the salinity anomaly method, though again there are greater uncertainties associated with the salinity model than the multi-tracer model. This may be indicative of the limitations of the salinity method to estimate shorter timescale residence times, as discussed earlier. The E-P data used for our calculations may be more representative of the platform average and less applicable to individual study sites, which may be affected by local rain or wind events. Nevertheless, it is encouraging that the salinity-based residence times are in good agreement with those estimated using the multi-tracer model. The greater certainty associated with the multi-tracer model, however, makes it a more ideal approach for estimating residence times in high energy reef environment like the Bermuda reef platform.

We can also evaluate the model's success by assessing output particle scavenging values (Kp). Previous studies show particle flux in the Sargasso Sea, the offshore water that flushes the Bermuda reef platform, varies over seasonal and intraannual timescales (Brzekinski and Nelson 1995; Conte et al. 2001). Overall, results from this study show larger Kp values at the rim reef and lower values closer toward shore (Table 2). This is in agreement with previous work from Muir et al. (2005), who saw shorter residence times (i.e., larger Kp) of ²³⁴Th in sea water further from shore (about 3 d) and longer suspension times (i.e., smaller Kp) closer to shore (about 9 d). Other studies have shown that Kp is positively related to water velocity, therefore systems with higher velocities correspond with high Kp values (Gustafsson et al. 1998; Savoye et al. 2006). Though current meter data does not exist for our study sites, it is likely that the rim reef (NR) experiences higher reef water velocities than more isolated sites closer to shore (B33), thus the corresponding higher Kp values at NR and lower Kp at B33 agree with these earlier studies.

NEC rates

Platform-average and site-specific NEC rates calculated from the alkalinity anomaly method (Eq. 2) using modeled residence times are shown in Fig. 9. NEC rates across all study sites were greater in November when ocean waters maintained late summer characteristics (e.g., temperature, light) with platformaverage rates of 20.3 (± 7.0) and 20.5 (± 5.7) mmolCaCO₃ m⁻² d⁻¹ in 2008 and 2009, respectively, compared with NEC rates of 2.5 (\pm 0.5) and 6.4 (\pm 1.5) mmolCaCO $_3$ m $^{-2}$ d $^{-1}$ in February of 2009 and March of 2010, respectively (Fig. 9). These results are consistent with increased calcification rates typically observed in coral reef systems during months with warmer sea surface temperatures and longer daylight hours (Logan et al. 1994; Bates et al. 2010). These results also support the argument that the diminished contrast between offshore and reef water TA data in February and March compared with November results is a results of diminished wintertime calcification and not reduced exchange rates as suggested by the ⁷Be tracer (Fig. 5).

Among individual sites, NR and MDP, having the greatest coral coverage, had the greatest calcification rate, with



November 2008 February 2009 November 2009 March 2010

Fig. 9. Spatial range of reef water residence times footprints. Lines represent the minimum ($U = 3.5 \text{ cm s}^{-1}$) and maximum ($U = 15 \text{ cm s}^{-1}$) footprint averaged over each of the four sampling periods. Effects of local environments were considered to help restrain the boundaries within the northern platform (i.e. shoreline and platform edge). Modifications to the estimated footprint radius at B33 were also made, confining the footprint within the southwestern lagoon.

November results ranging from 77.9 (± 7.6) mmolCaCO₃ $m^{-2}d^{-1}$ to 101.6 (± 14.3) mmolCaCO₃ $m^{-2}d^{-1}$ compared with inshore patch reefs such as B33 which ranged between 31.8 (± 7.9) mmolCaCO $_3$ m⁻²d⁻¹ to 37.3 (± 6) mmolCaCO $_3$ m⁻²d⁻¹ and Pylon, which ranged between 37.3 (\pm 9.0) mmolCaCO $_3$ m $^{-2}$ d $^{-1}$ to 38.0 (± 10) mmolCaCO₃ m⁻²d⁻¹ in November (CARICOMP 2002). Previous attempts to estimate NEC rates in Bermuda have been limited by the inability to accurately estimate reef water residence times. Bates et al. (2010) however report NEC rates ranging from a winter low of -20.9 mmolCaCO₃ m⁻²d⁻¹ to a summer time maximum of about 100 mmolCaCO₃ m⁻²d⁻¹ at Hog Reef, a rim reef with a benthic community comparable to North Rock. In Bates' study NEC rates were estimated assuming an average reef depth of 6 m and residence time of 2 days coupled with offshore and onshore TA data. The gap in Bates' study from January to April is complemented by the February and March data provided here.

For further comparison, Bates et al. (2010) also provide estimates of NEC rates scaled-up from in situ skeletal growth rates measurements at Hog Reef which, assuming a live coral coverage of 50%, yield NEC rates ranging from 42.8 mmolCaCO $_3$ m $^{-2}$ d $^{-1}$ to 105.7 mmolCaCO $_3$ m $^{-2}$ d $^{-1}$. These results are again within the range observed in this study at NR and MDP, reefs with comparable coral coverage.

In this comparison however, it is important to note that results from this study represent the platform integrated signal for each study area because water samples were collected inbetween reefs and not directly over the reef. Though the observed ⁷Be activity is probably not affected by this sampling method, changes in TA over the reef are likely different than those observed in this study. The result of this approach is a

more accurate estimate of the platform integrated NEC rate for each sampling area; though in order to fully appreciate the value of these results this sampling area, or model "footprint," must be explicitly defined.

Spatial resolution (the model "footprint")

Can a site-specific approach, more highly resolved than the average platform consideration, be justified?

Water samples were collected adjacent to the reef, as opposed to directly over the reef, and thus represent the integrated platform signal of an undefined spatial range. To quantify this range and assess the ability of our model to resolve local (site-specific) residence times and NEC rates, we must quantify the model's spatial range (or footprint). This can be evaluated with the tracer response time, as discussed above (Eq. 5). Tracer response times are on the same order of magnitude as the estimated site-specific residence times (Table 2), indicating that the tracers are responding at an appropriate timescale to estimate the local residence time. Model footprints can then be estimated from these tracer response time and measurements of local reef water velocity.

Reef water velocity data are limited for the Bermuda reef platform, but data from Hog reef, a rim reef site similar to NR, show typical velocities between 10-15 cm s⁻¹ with occasionally higher speeds of 25-35 cm s⁻¹. These faster velocities, however, may be restricted to rim reef sites like Hog reef and NR where water is more rapidly exchanged with offshore water compared to more isolated sites such as Pylon or B33. In the absence of measured reef water velocities at our sampling sites, we used published data, and assess our footprints with a minimum velocity of 3.5 cm s⁻¹ and a maximum velocity of 15 cm s⁻¹ (Morris et al. 1977; Mills et al. 2005). The product of reef water velocity and tracer response time (Eq. 5) was then used

to estimate the radius or "footprint" of our tracers from each sampling site (Table 5, Fig. 10).

Estimating the tracers' spatial limit provides a means to resolve the spatial boundaries of modeled residence times and thus define the sampling area. Becuase the serial box model does not assume the history of a given water parcel from its onset to the reef platform, the model's spatial range can theoretically circulate from the sampling location, and not from the platform edge. This approach however only provides a uniform radius centered at the study site, which may be unrealistic con-

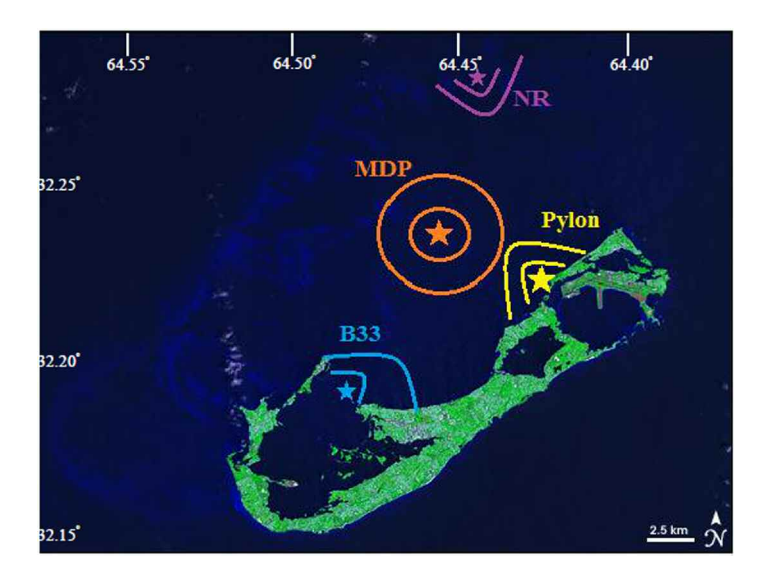


Fig. 10. Platform-average (black) and site-specific (gray) NEC rates estimated according to the alkalinity anomaly method using modeled residence times. Results are given for the biannual seasonal study from Nov 2008 to Mar 2010.

Table 5. Model footprints, defined as the product of tracer response times (Table 2) and reef water velocity calculated here with a maximum velocity of 15.0 cm s⁻¹ and minimum velocity of 3.5 cm s⁻¹, thus yielding a minimum and maximum range of site specific model footprints.

		U = 3.5 cm s ⁻¹		U = 15 cm s ⁻¹	
Date	Site	Minimum footprint (km)	±	Maximum footprint (km)	±
Nov 08	NR	0.11	0.07	0.45	0.02
	Pylon	0.23	0.02	0.97	0.01
	B33	0.30	0.05	1.30	0.01
Feb 09	NR	0.13	0.03	0.54	0.01
	Pylon	0.45	0.10	1.95	0.06
	B33	0.45	0.10	1.95	0.07
Nov 09	NR	0.13	0.03	0.54	0.01
	MDP	0.20	0.03	0.86	0.01
	Pylon	0.17	0.03	0.71	0.01
	B33	0.42	0.01	1.79	0.09
Mar 10	NR	0.25	0.03	1.08	0.01
	MDP	0.46	0.03	1.99	0.14
	Pylon	0.71	0.40	3.03	0.15
	B33	0.55	0.42	2.38	0.12

sidering local geographic constraints. Spherical footprints were therefore adjusted based on physical restrictions dictated by local environments (Fig. 10). Footprints were confined to the boundaries of the northern platform and did not extend past the platform edge or into the southern platform, thereby constraining the footprints at NR and Pylon. Furthermore, the footprints estimated for B33 were confined within the southwestern bay and did not extend uniformly outside the bay.

Error analysis

As mentioned earlier, the model's ability to estimate reef water residence time is limited by analytical error of measured model parameters (${}^{7}\text{Be}_{\text{R}}$, ${}^{7}\text{Be}_{\text{Q}}$, ${}^{7}\text{Be}_{\text{p}}$, ${}^{234}\text{Th}_{\text{R}}$, ${}^{234}\text{Th}_{\text{Q}}$, ${}^{234}\text{Th}_{\text{p}}$, F, z). Here we discuss the significance of each parameter's analytical uncertainty and the corresponding impact to the overall uncertainty of modeled reef water residence times and NEC. Specifically, we focus on sensitivity to variability in atmospheric flux of ${}^{7}\text{Be}$ from rainfall (F), the assumed 10 m reef depth (z), tracer sinks (Kp), and analytically derived tracer activities, assessing the role of these assumptions and uncertainties to the overall model output residence times and corresponding NEC rates.

To assess the atmospheric flux of ^7Be from rainfall, we allowed this parameter to vary from 250-650 dpm m $^{-2}$ d $^{-1}$ based on the range observed during our study (Fig. 11). By running the model for this range in F, we show that estimated residence times only vary by 6% to 18%, well within the model's margin of error (Fig. 12). The reason is that the rain flux over the reef (F/z) only accounts for only 9% to 17% of the ^7Be input compared to exchange with offshore water ($^7\text{Be}_\text{Q}/\tau$) which account for the remaining 91% to 83% (Table 6, 7).

Activities of ⁷Be and ²³⁴Th in seawater are generally measured to an accuracy of 7% while activities on particles are between 10% to 15%. As discussed earlier, ⁷Be fiber efficiency typically ranges between 76% to 82% for extraction of ⁷Be from sea water. Greater uncertainty in particulate activities stems from the multi-step extraction process, described above. These analytical error account for roughly 15% of the total uncertainty in modeled residence times (Table 6).

Uncertainty of the reef depth (z) has a significantly larger impact. As discussed earlier, we assume a universal 10 m depth across the reef platform and for each of our study sites. The purpose of this was to estimate a spatially and temporally averaged residence time and NEC. Water samples were collected adjacent to the reefs to capture this spatial average, which likely affects nTA more than radiochemical sampling. In accordance with this spatially averaged water sample, we need to assume an average reef depth over the same range represented by our water samples. To date there are no bathymetry data for the Bermuda reef platform at the resolution required for this project (see for example however http://dnc.nga.mil/NGAPortal/DNC.portal for limited available data). Average depths range from 8 to 18 m (Stanley and Swift 1968), though depths over reefs can be much shallower

(>1 m). The high variability in bathymetry across the platform, and even within the model's footprint for each site, can potentially generate large uncertainty in z. The model's assumed 10 m depth represents the average for the area encompassed by the model's footprint, the uncertainty associated with this variable is dependent on the limited bathymetry data for the given area. For example, the 0.11-1.08 km footprint around NR encompasses roughly 45% of shallow (<10 m) fringing reef, thus we assumed an uncertainty of 4.5m at this site.

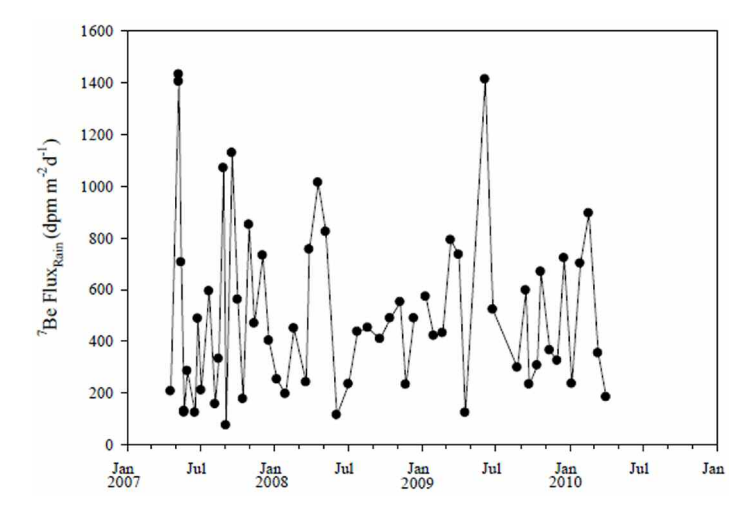


Fig. 11. Atmospheric flux of ⁷Be from rainfall collected from the Bermuda Institute of Ocean Sciences between Aug 2007 and Apr 2010. Collection periods ranged from 3-6 weeks based on the amount of accumulated rainfall.

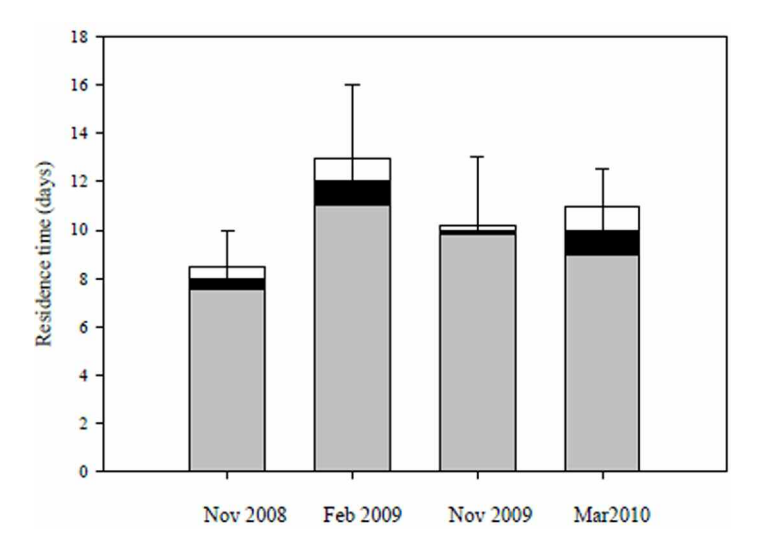


Fig. 12. Platform-average residence time and model uncertainty (black) with the maximum (white) and minimum (gray) residence times resulting from a rain flux variation of 250-650 dpm m⁻² d⁻¹. The minimal impact of this range of rain flux (6%-18%) on the overall uncertainty of the residence time helps validate the assumed monthly average rain flux used in this model.

Table 6. Measured activities and corresponding analytical uncertainties of each model parameter. Analytical uncertainty of ⁷Be and ²³⁴Th in seawater account for roughly 7% of the model uncertainty whereas ⁷Be and ²³⁴Th on particles accounts for 10% to 15%. Though analytical uncertainty in the rain flux is also roughly 7%, the assumed steady state monthly flux used in the model generates a slightly larger contribution to the overall model uncertainty, roughly 18%.

		⁷ Be _R		²³⁴ Th _R		⁷ Be _₽		²³⁴ Th _p		F _{rain}	
Date	Site	(dpm L ⁻¹)	±	(dpm L ⁻¹)	±	(dpm L ⁻¹)	±	(dpm L ⁻¹)	±	(dpm m ⁻² d ⁻¹)	±
Nov 08	Off Shore	607	29	2557	94					550	39
	NR	498	36	990	33	250	34	334	32	550	39
	Pylons	485	29	539	26	350	45	193	21	550	39
	B33	674	38	352	13	320	4	515	56	550	39
Feb 09	Off Shore	247	32	2340	115					421	29
	NR	227	33	1874	76	70	20	132	76	421	29
	Pylons	421	29	813	56	227	43	179	42	421	29
	B33	399	41	402	28	210	30	170	4	421	29
Nov 09	Off Shore	558	27	1963	84					365	26
	NR	456	34	619	42	87	20	156	4	365	26
	MDP	495	37	435	45	335	37	111	4	365	26
	Pylons	459	33	245	41	158	31	102	3	365	26
	B33	787	38	238	55	188	28	101	4	365	26
Mar 10	Off Shore	211	9	2453	106					309	22
	NR	212	18	502	29	125	28	1 <i>7</i> 1	6	309	22
	MDP	398	22	496	41	149	27	286	28	309	22
	Pylons	673	28	469	40	172	26	235	8	309	22
	B33	731	29	796	27	308	31	243	7	309	22

Table 7. A comparison of model inputs from offshore flushing and rain. The model is more sensitive to offshore flushing which is typically 2-4 times greater than the rain ⁷Be input from rain.

Date	Site	$^7\mathrm{Be}_\mathrm{Q}/ au$	F_{rain}/z
Nov 08	Average	75.88	55.0
	NR	433.57	55.0
	Pylon	151.75	55.0
	B33	67.44	55.0
Feb 09	Average	20.58	42.1
	NR	109.78	42.1
	Pylon	70.57	42.1
	B33	35.29	42.1
Nov 09	Average	55.80	36.5
	NR	248.00	36.5
	MDP	186.00	36.5
	Pylon	111.60	36.5
	B33	46.50	36.5
Mar 10	Average	21.10	30.9
	NR	46.89	30.9
	MDP	42.20	30.9
	Pylon	35.17	30.9
	B33	23.44	30.9

The uncertainty in each model parameter contributes to the overall uncertainty of the modeled residence time. To quantify this uncertainty in τ we assess how the model responds to parameter input values that vary by their respective uncertainties (ie, measured value \pm analytical uncertainty). This produces the range in modeled residence times associated with the uncertainty of each model parameter. This range is then used to define the overall uncertainty in our modeled residence time.

The overall uncertainty of modeled reef water residence times, reef depth, and analytical error of measured nTA are incorporated into the overall uncertainty of estimated NEC (Table 8). Analytical uncertainty in nTA is typically within 2%, thus most of the uncertainty in NEC derives from the modeled residence times and assumed reef depth. As discussed earlier, uncertainty in reef depth is derived from limited bathymetry data within each model footprint, and uncertainty of reef water residence times stems from analytical uncertainty attributed to each model parameters. Both contribute significantly to the overall uncertainty of NEC with reef depth ranging from 10% to 45% and residence time ranging from 27% to 50% (Table 7).

Model sensitivity

Though the model's accuracy is limited by analytical uncertainty, the model's sensitivity to Kp, τ and λ can reveal which parameters are controlling the 7Be and ^{234}Th activity of the system. Kp and τ are competing with λ and will have a stronger influence on the system if larger than λ (or, in the case of τ , $1/\tau$

Table 8. Parameters used to estimate NEC: salinity normalized total alkalinity (S = 35.00), modeled reef water residence times and assumed reef depth of each sampling site during the 2 years bi-seasonal study. nTA is generally measured within 2%, and therefore, contributes minimally to the overall uncertainty of NEC. Modeled reef water residence times and reef depth account for the majority of the uncertainty.

Date	Site	nTA (µmol kg ⁻¹)	±	Residence time (d)	±	Reef depth (m)	±
Nov-08	Off Shore	2297	46			10	1
	NR	2258	45	1.4	0.7	10	4.5
	Pylons	2252.9	41	4	1.3	10	3.3
	B33	2217	44	9	4	10	2.5
Feb-09	Off Shore	2282	46			10	1
	NR	2285	51	2.25	0.8	10	4.5
	Pylons	2278	46	3.5	1	10	3.3
	B33	2276	68	7	2	10	2.5
Nov-09	Off Shore	2290	46			10	1
	NR	2255	53	2.25	0.9	10	4.5
	MDP	229	5	3	0.9	10	3.3
	Pylons	2253	45	5	1.8	10	3.3
	B33	2214	44	12	4	10	2.5
Mar-10	Off Shore	2296	69			10	1
	NR	2280	46	4.5	1.2	10	4.5
	MDP	2281	48	5	1.75	10	3.3
	Pylons	2287	46	6	1.9	10	3.3
	B33	2288	42	9	3	10	2.5

 $> \lambda$). Generally results show Kp $> \lambda$ for both ^7Be ($\lambda = 0.013 \text{ d}^{-1}$) and ^{234}Th ($\lambda = 0.02876 \text{ d}^{-1}$), indicating that the system is responding more to particle scavenging than radioactive decay (Table 2). Similarly, $1/\tau > \lambda$ for both tracers, again indicting that the system is responding more to the residence time than radioactive decay (Table 2). Thus, for the short residence times of this reef system, the activities of ^7Be and ^{234}Th in reef water appear to be more sensitive to Kp and τ and less responsive to radioactive decay.

Comments and recommendations

The novel method for estimating reef water residence times presented here has also been applied to coral reefs in Puerto Rico and the Florida Keys as part of this same study. A comparison paper, currently in preparation, will describe how the rates of NEC obtained by the ⁷Be residence time/alkalinity anomaly method compare with rates based on Eulerian, Lagrangian, and enclosure methods. The advantage of the ⁷Be method is that it yields a temporally and spatially averaged rate of NEC. The other methods yield instantaneous rates and require a lot of labor intensive sampling in order to achieve a temporally and spatially averaged estimate of NEC rates.

The ⁷Be method may be compromised in environments where rivers, streams, or ground water input could deliver ⁷Be to the study site. The ⁷Be activity of these sources and removal rate from particles would have to be quantified if the ⁷Be method is to be accurately applied in these environments. The ⁷Be method may also be compromised during summer months

due to shoaling of the offshore mixed layer that diminishes the required contrast in ⁷Be activities between offshore and reef water. In the Bermuda study, we were quite conservative in only sampling at times of the year when the mixed layer depth offshore was much greater than the average water depth over the reef. For our subsequent studies in Puerto Rico and the Florida Keys, we relaxed this restriction and still obtained reasonable residence times and NEC rates sampling at times of the year when the mixed layer depth offshore was as little as 20 m.

The ⁷Be method provides a means to quantify NEC rates in high energy reef environments where estimates have previously been limited due to an inability to accurately estimate reef water residence times. In light of recent declines in ocean pH these estimates are becoming of increasing importance. They provide a means to assess how coral communities are responding to pressures attributed to global climate change and ocean acidification by establishing baseline NEC rates against which future recovery or decline can be assessed.

References

Akata, N., and others. 2007. Total deposition velocities and scavenging ratios of ⁷Be and ²¹⁰Pb at Rokkasho, Japan. J. Radioanal. Nucl. Chem. 77:347-355 [doi:10.1007/s10967-007-7095-1].

Andersson, A. J., I. B. Kuffner, F. T. Mackenzie, P. L. Jokiel, K. S. Rodgers, and A. Tan. 2009. Net loss of CaCO₃ from a subtropical calcifying community due to seawater acidifica-

- tion: mesocosm-scale experimental evidence. Biogeosciences 6:1811-1823 [doi:10.5194/bg-6-1811-2009].
- ——, F. T. Mackenzie, and J. -P. Gattuso. 2011. Effects of ocean acidification on benthic processes, organisms, and ecosystems, p. 122-153. *In* J. -P. Gattuso and L. Hansson [eds.], Ocean acidification. Oxford Press.
- Andréfouët, S., J. Pagès, and B. Tratinville. 2001. Water renewal time for classification of atoll lagoons in the Tuamotu Archipelago (French Polynesia). Coral Reefs 20:399-408 [doi:10.1007/s00338-001-0190-9].
- Baker, A. C., P. W. Glynn, and B. Riegl. 2008. Climate change and coral reef bleaching: An ecological assessment of longterm impacts, recovery trends and future outlook. Estuar. Coast. Shelf Sci. 80:435-471 [doi:10.1016/j.ecss.2008. 09.003].
- Bates, N. R. 2007. Interannual variability of the oceanic CO₂ sink in the subtropical gyre of the North Atlantic Ocean over the last 2 decades. J. Geophys. Res. Oceans 112:C09013 [doi:10.1029/2006JC003759].
- ——, A. F. Michaels, and A. H. Knap. 1996a. Seasonal and interannual variability of the oceanic carbon dioxide system at the US JGOFS Bermuda Atlantic Time-series Site. Deep-Sea Res. II 43:347-383 [doi:10.1016/0967-0645(95)00093-3].
- ——, A. F. Michaels, and A. H. Knap. 1996b. Alkalinity changes in the Sargasso Sea: geochemical evidence of calcification? Mar. Chem. 51:347-358 [doi:10.1016/0304-4203(95)00068-2].
- —, A. Amat, and A. J. Andersson. 2010. The interaction of carbonate chemistry and coral reef calcification: the carbonate chemistry coral reef ecosystem feedback (CREF) hypothesis. Biogeosciences 7:2509-2530 [doi:10.5194/bg-7-2509-2010].
- ——, M. H. P. Best, K. Neely, R. Garley, A. G. Dickson, and R. J. Johnson. 2012. Detecting anthropogenic carbon dioxide uptake and ocean acidification in the North Atlantic Ocean. Biogeosciences 9:2509-522 [doi:10.5194/bg-9-2509-2012].
- Bhat, S., G. Krishnaswamy, A. Lal, A. D. Rama, and W. Moore. 1969. ²³⁴Th/²³⁸U ratios in the ocean. Earth Planet. Sci. Lett. 5:483-491 [doi:10.1016/S0012-821X(68)80083-4].
- Brahmi, C., and others. 2010. Skeletal growth, ultrastructure and composition of the azooxanthellate scleractinian coral Balanophyllia *regia*. Coral Reefs 29:175-189 [doi:10.1007/s00338-009-0557-x].
- Broecker, W. S., A. Kaufman, and R. M. Trier. 1973. The residence time of thorium in surface sea water and its implications regarding the rate of reactive pollutants. Earth Planet. Sci. Lett. 20:35-44 [doi:10.1016/0012-821X(73)90137-4].
- Brzekinski, M. A., and M. D. Nelson. 1995. The annual silica in the Sargasso Sea near Bermuda. Deep Sea Res. I 4:1215-1237 [doi:10.1016/0967-0637(95)93592-3].
- Butler, J. N. 1992. Alkalinity titration in seawater- how accurately can the data be fitted by and equilibrium model. Mar.

- Chem. 38:251-282 [doi:10.1016/0304-4203(92)90037-B].
- CARICOMP (25 co-authors). 2002. Status and temporal trends at CARICOMP coral reef sites. *In* Soekarno and Suharsono [Eds.]. Proceedings of the Ninth International Coral Reef Symposium, Bali. 23–7 Oct 2000.
- Chalker, B., D. Barnes, and P. Isdale. 1985. Calibration of x-ray densitometry for the measurement of coral skeletal density. Coral Reefs 4:95-100 [doi:10.1007/BF00300867].
- Coale, K. H., and K. W. Bruland. 1985. ²³⁴Th:²³⁸U disequilibria within the California Current. Limnol. Oceanogr. 30:22-33 [doi:10.4319/lo.1985.30.1.0022].
- Conte, M. H., N. Ralph and E. H. Ross. 2001. Seasonal and interannual variability in deep ocean particle fluxes at the Oceanic Flux Program(OFP) Bermuda Atlantic Time Series (BATS) site in the south west Sargasso Sea near Bermuda. Deep Sea Res. II 48:1471-1505 [doi:10.1016/S0967-0645(00)00150-8].
- Cooper, L. W., I. L. Larsen, J. M. Grebmeier, and S. B. Moran. 2005. Detection of rapid deposition of sea ice-rafted material to the Arctic Ocean benthos using the cosmogenic tracer 7Be. Deep-Sea Res. II 52:3452-3461 [doi:10.1016/j.dsr2.2005.10.011].
- De'ath, G., J. M. Lough, and K. E. Fabricius. 2009. Declining coral calcification on the Great Barrier Reef. Science 323:116-119 [doi:10.1126/science.1165283].
- Delesalle, B., and A. Sournia. 1992. Residence time of water and phytoplankton biomass in coral reef lagoons. Cont. Shelf Res. 12:939-949 [doi:10.1016/0278-4343(92)90053-M].
- Dickson, A. G., J. D. Afghan, and G. C. Anderson. 2003. Reference materials for oceanic CO_2 analysis: a method for the certification of total alkalinity. Mar. Chem. 80:185-197 [doi:10.1016/S0304-4203(02)00133-0].
- Dikou, A. 2009. Skeletal linear extension rates of the foliose scleractinian coral Merulina *ampliata* (Dllis & Solander, 1786) in a turbid environment. Mar. Ecol. 30:405-415.
- Dore, J. E., R. Lukas, D. W. Sadler, M. J. Church, and D. M. Karl. 2009. Physical and biogeochemical modulation of ocean acidification in the central North Pacific. Proc. Natl. Acad. Sci. U.S.A. 106:12235-12240 [doi:10.1073/pnas.0906 044106].
- Gardner, T. A., I. M. Côté, J. A. Gill, A. Grant, and A. R. Watkinson. 2003. Long-term region-wide declines in Caribbean corals. Science 301:958-960 [doi:10.1126/science.1086050].
- Gattuso, J.- P., M. Frankignoulle, I. Boutge, S. Romaine, and R. W. Buddemeier. 1998. Effect of calcium carbonate saturation of seawater on coral calcification. Global Planet. Change 18:37-46 [doi:10.1016/S0921-8181(98)00035-6].
- Glynn, P. W. 1990. Coral mortality and disturbances to coral reefs in the tropical eastern Pacific. Global Ecological Consequences of the 1982-1983 El Nino-Southern Oscillation. 5:5-126.
- Gray, S. E., M. D. DeGrandpre, C. Langdon, and J. E. Corredor. 2012. Short term and seasonal pH, pCO_2 , and saturation state variability in a coral reef ecosystem. Global Bio-

- geochem. Cycles 26:GB3012 [doi:10.1029/2011GB004114].
- Gustafsson, Ö., K. O. Buesseler, W. R. Geyer, S. B. Moran, and P. M. Gschwend. 1998. An assessment of the relative importance of horizontal and vertical transport of particle-reactive chemicals in the coastal ocean. Cont. Shelf Res. 18:8005-829 [doi:10.1016/S0278-4343(98)00015-6].
- Haus, B. K., J. D. Wang, J. Rivera, J. Martinez-Pedraja, and N. Smith. 2000. Remote radar measurement of shelf currents off Key Largo, FL, USA. Estuar. Coast. Shelf Sci. 51:553-569 [doi:10.1006/ecss.2000.0704].
- Hofmann, G. E., and others. 2011. High-frequency dynamics of ocean pH a multi-ecosystem comparison. PLOS One 6:12 [doi:10.1371/journal.pone.0028983].
- Hoegh-Gulberg, O., and others. 2007. Coral reefs under rapid climate change and ocean acidification. Science 318:1737-1742 [doi:10.1126/science.1152509].
- IPCC. Solomon, S., and others [eds.]. 2007. Climate change 2007: The physical science basis. Contribution of Working Group I to the Fourth Assessment Report of the Intergovernmental Panel on Climate Change. Cambridge Univ. Press.
- Kadko, D. 2000. Modeling the evolution of the arctic mixed layer during the fall 1997 SHEBA project using measurements of ⁷Be. Journal of Geophysical Research 105:3369-3378 [doi:10.1029/1999JC900311].
- 2009. Rapid oxygen utilization in the ocean twilight zone assessed with the cosmogenic isotope ⁷Be. Global Biogeochemical Cycles 23:GB4010 [doi:10.1029/2009GB003510].
- ——, and D. Olson. 1996. Be-7 as a tracer of surface water seduction and mixed layer history. Deep Sea Res. 43:89-116 [doi:10.1016/0967-0637(96)00011-8].
- ——, and J. Prospero. 2011. Deposition of ⁷Be to Bermuda and the regional ocean: Environmental factors affecting estimates of atmospheric flux to the ocean. J. Geophys. Res. 116:C02013 [doi:10.1029/2010JC006629].
- Kayanne, H., and others. 2005. Seasonal and bleaching-induced changes in coral reef metabolism and CO2 flux. Global Biogeochem. Cycles 19:GB3015 [doi:10.1029/2004 GB002400].
- Langdon, C., and others. 2003. Effect of elevated ${\rm CO_2}$ on the community metabolism of an experimental coral reef. Global Biogeochem. Cycles 17:1-14 [doi:10.1029/2002 GB001941].
- ——, and M. J. Atkinson. 2005. Effect of elevated pCO_2 on photosynthesis and calcification of corals and interactions with seasonal change in temperature/irradiance and nutrient enrichment. J. Geophys. Res. 110:1-16, C09S07 [doi:10.1029/2004JC002576].
- ——, J. -P. Gattuso, and A. J. Andersson. 2010. Measurements of calcification and dissolution of benthic organisms and communities, p. 155-174. *In* U. Riebesell, V. J. Fabry, L. Hansson, and J. -P. Gattuso [eds.], Guide to best practices in ocean acidification research and data reporting. Office for official publications of the European Communities.

- Lee, T., E. Barg, and D. Lal. 1991. Studies of vertical mixing in the Southern California Bight with cosmogenic radionuclides ³²P and ⁷Be. Limnol. Oceanogr. 365:1044-1053 [doi:10.4319/lo.1991.36.5.1044].
- Logan, A., L. Yang, and T. Tomascik. 1994. Linear skeletal extension rates in two species of Diploria from high-latitude reefs in Bermuda. Coral Reefs 13:225-230 [doi:10.1007/BF00303636].
- Manzello, D. P. 2010. Ocean acidification hotspots: Spatiotemporal dynamics of the seawater CO2 system of eastern Pacific coral reefs. Limnology and Oceanography 55:239-248 doi:10.4319/lo.2010.55.0239
- Mills, M. M., F. Lipschultz, and K. P. Sebens. 2005. Particulate matter ingestion and associated nitrogen uptake by four species of scleractinian coral. Coral Reefs 23:311-323 [doi:10.1007/s00338-004-0380-3].
- Moran, S. B., H. N. Edmonds, J. N. Smith, R. P. Kelly, M. E. Q. Pilson, and W. G. Harrison. 2003. Does ²³⁴Th/²³⁸U disequilibrium provide an accurate record of the export flux of particulate organic carbon from the upper ocean? Limnol. Oceanogr. 48:1018-1029 [doi:10.4319/lo.2003.48.3.1018].
- Morris, B., J. Barnes, F. Brown, and J. Markham. 1977. The Bermuda marine environment: a report of the Bermuda Inshore Waters Investigations 1976-1977. Special Publ. Bermuda Biol. Station Res. 15:1–189.
- Muir, G. K. P., J. M. Pates, A. P. Karageorgis, and H. Kaberi. 2005. ²³⁴Th:²³⁸U disequilibrium as an indicator of sediment resuspension in Thermaikos Gulf, northwestern Aegean Sea. Cont. Shelf Res. 25:2476-2490 [doi:10.1016/j.csr. 2005.08.009].
- Orr, J. C. 2011. Recent and future changes in ocean carbonate chemistry, p. 41-66. *In J.- P. Gattuso and L. Hansson [eds.]*, Ocean acidification. Oxford Press.
- Pandolfi, J. M., and others. 2005. Are U.S. coral reefs on the slippery slope to slime? Science 207:1725-1726 [doi:10.1126/science.1104258].
- Prandle, D. 1984. A modeling study of the mixing of Cs-137 in the seas of the European Continental-Shelf. Phil. Trans. R. Soc. Lond. 310:407-436 [doi:10.1098/rsta.1984.0002].
- Sakurai, H., Y. Shouji, M. Osaki, T. Aoki, T. Gandou, W. Kato, and Y. Takahashi. 2005. Relationship between daily variation of cosmogenic nuclide Be-7 concentration in atmosphere and solar activities. Adv. Space Res. 36:2492-2496 [doi:10.1016/j.asr.2003.08.083].
- Savoye, N., and others. 2006. ²³⁴Th sorption and export models in the water column: A review. Mar. Chem. 100:234-249 [doi:10.1016/j.marchem.2005.10.014].
- Schneider, K., and J. Erez. 2006. The effect of carbonate chemistry on calcification and photosynthesis in the hermatypic coral *Acropora eurystoma*. Limnol. Oceanogr. 51:1284-1293 [doi:10.4319/lo.2006.51.3.1284].
- Silker, W. B. 1972. Beryllium-7 and fission products in the GEOSECS II water column and applications of their oceanic distributions. Earth Planet. Sci. Lett. 16:131-137

[doi:10.1016/0012-821X(72)90247-6].

- Silverman, J., B. Lazar, and J. Erez. 2007. Effect of aragonite saturation, temperature and nutrients on the community calcification rate of a coral reef. J. Geophys. Res. 112:C5:C05004.
- ——, and others. 2012. Carbon turnover rates in the One Tree Island reef: A 40 year perspective. J. Geophys. Res. 117:G03023 [doi:10.1029/2012]G001974].
- Smith, S. V. 1973. Carbon dioxide dynamics: a record of organic carbon production, respiration and calcification in the Eniwetok reef flat community. Limnol. Oceanogr. 18:106-120 [doi:10.4319/lo.1973.18.1.0106].
- ———, and F. Pesret. 1974. Processes of carbon dioxide flux in the Fanning Island Lagoon. Pac. Sci. 28:225-245.
- ———, and P. L. Jokiel. 1978. Water composition and biogeochemical gradients in the Canton Atoll lagoon. Atoll Res. Bull. 221:17-53.
- Stanley, D. J., and D. J. P. Swift. 1968. Bermuda's reef-front platform bathymetry and significance. Mar. Geol. 6:479-500 [doi:10.1016/0025-3227(68)90028-5].
- Yates, K. K., C. Dufore, N. Smiley, C. Jackson, and R. B. Halley. 2007. Diurnal variations of oxygen and carbonate system

- parameters in Tampa Bay and Florida Bay. Mar. Chem. 104:110-124 [doi:10.1016/j.marchem.2006.12.008].
- Waddell, J. E., and A. M. Clarke [eds.]. 2008. The state of coral reef ecosystems of the United States and Pacific Freely Associated States: 2008. NOAA Technical Memorandum NOS NCCOS 73. NOAA/NCCOS Center for coastal monitoring and assessments biogeography team.
- Wantanabe, A., and others. 2006. Analysis of the seawater CO₂ system in the barrier reef-lagoon system of Palau using total alkalinity-dissolved inorganic carbon diagrams. Limnol. Oceanogr. 5:1614-1628 [doi:10.4319/lo.2006.51.4.1614].
- Wilkinson, C., and A. Bernard. 2012. Coastal resource degradation in the tropics: does the tragedy of the commons apply for coral reefs, mangrove forests and seagrass beds? Mar. Poll. Bull. 64:1096-1105 [doi:10.1016/j.marpolbul.2012.01.041].
- Zeebe, R. E., and D. Wolf-Gladrow. 2001. CO₂ in seawater: equilibrium, kinetics, isotopes, 1st ed. Elsevier.

Submitted 25 April 2012 Revised 26 November 2012 Accepted 31 December 2012